CHEMICAL ENGINEERING TRANSACTIONS
VOL. 68, 2018
A publication of AIDIC
The Italian Association of Chemical Engineering
Online at www.aidic.it/cet
Guest Editors: Selena Sironi, Laura Capelli

ISBN 978-88-95608-65-5; **ISSN** 2283-9216
DOI: 10.3303/CET1868079

Pt/Pd-Fe_3O_4 Nanoparticles for Removal of Humic Acids and Cr(VI)

Maria Sarno*, Eleonora Ponticorvo

Department of Industrial Engineering and Centre NANO_MATES University of Salerno, Via Giovanni Paolo II ,132 - 84084 Fisciano (SA), Italy
msarno@unisa.it

Dumbbell-like Pt/Pd-Fe_3O_4 nanoparticles (NPs) for the effective and simultaneous removal of Humic Acids and Cr (VI) have been prepared by a one-step synthetic approach. The NPs after a ligand exchange process result suitable to be dispersed in water, electrochemical tests were carried out in a batch electrochemical cell. The NPs show excellent removal efficiency for total Cr. In particular ~ 64% of total Cr was removed in 30 min, while ~ 95 % of total Cr was removed in 9 h. Moreover, the complete removal of Cr (VI) was achieved in 1.5 h. Furthermore, they result able to remove ~ 95% of TOC after 9 h electrolysis, indicating a quite complete mineralization to CO_2 of HAs.

1. Introduction

Among the most widely distributed natural organic matters Humic acids (HAs) are ubiquitous in aquatic and soil environments, and constitute pollutants of soil, water and air (Sutton et al., 2005). These substances come from chemical and biochemical reactions occurring during humification of organic matters (Trellu et al., 2016). They are complex and heterogeneous mixtures of aromatic macromolecules, having functionality such as carboxylic, phenolic, alcoholic, ketone and quinone groups (Trellu et al., 2016). As a consequence, HAs play important roles in the aquatic systems: as adsorbents for removal of many toxic trace metals and organic pollutants such as herbicides and pesticides and as reductants for initiating electron transfer to high oxidation states of heavy metals and organic chlorinated contaminants (Wiszniowski et al., 2002). On the other hand, the existence of HAs in drinking water may lead to color, taste and odor problems, and to biological instability of drinking water in distribution system (Wang et al., 2016). Moreover, these compounds are widely recognized as precursors for potentially carcinogenic disinfection by-products (DBPs), e.g. trihalomethanes formation during chlorine disinfection process (Trellu et al., 2016). Therefore, the removal of HAs from drinking water sources is of great importance and strongly desired for the protection of public health.
Hexavalent chromium (Cr(VI)), produced in many industrial processes such as electroplating, leather tanning, pigment manufacturing and wood preservation, is considered to be the second most dominant heavy metal in natural environment (Celebi et al., 2016). Due to its severe health impacts of mutagenicity and carcinogenicity on human being, Cr (VI) has been classified as Group A inhalation carcinogen by US EPA and Group I human carcinogen by the IARC (International Agency for Research on Cancer) (Kaya et al., 2016), resulting into the strictly regulated Cr (VI) level in drinking water that must be lower than 0.05 mg/L (Celebi et al., 2016). In addition, as an anion Cr (VI) is ready to enter and migrate in the soil and aquatic environments, leading to a tremendous threat to water supply sources (e.g. surface water and groundwater).
On another side, the increasing uses of Cr in industries have led to a large amount of effluents that contain Cr (VI) (Celebi et al., 2016), which thus makes common the coexistence of HAs and Cr in natural water bodies. The widespread presence of HAs and Cr in aquatic systems and drinking water sources is a serious threat to the environment and human being. However, very few studies on the potential interaction and simultaneous removal of these two types of contaminants have been conducted. Different catalysts have been proposed and studied for the removal of HAs and Cr (VI) (Li et al., 2013). On the other hand, nanotechnology offers also in this field a real opportunity of innovation, supplying new structure and morphology able to increase catalytic activity and selectivity for the simultaneous removal of both humic acids and chromium.

Please cite this article as: Sarno M., Ponticorvo E., 2018, Pt/pd-fe3o4 nanoparticles for removal of humic acids and cr(vi), Chemical Engineering Transactions, 68, 469-474 DOI: 10.3303/CET1868079

Here we propose a dumbbell-like Pt/Pd-Fe_3O_4 nanoparticles (NPs) for the effective and simultaneous removal of HAs and Cr (VI). For the magnetic NPs synthesis an easy and scalable approach was used (Sarno et al., 2014; Sarno et al., 2016a). In particular, to favour the dispersion of the nanoparticles in the electrochemical medium a ligand exchange was designed and promoted. This approach allows to disperse a stable catalyst in the reaction medium, trying to approach a homogeneous catalysis. On the other hand, the main disadvantage of the homogeneous catalysis, i.e. the separation of the catalyst, will be overcome by simply applying a magnetic field allowing an easy separation. A comparison with Pd-Fe_3O_4 catalyst is reported, highlighting the role of Pt in increasing catalyst selectivity. The electron transfer and hydrogen atom transfer were found the fundamental aspect during HAs and Cr(VI) removal.

2. Experimental

HAs were purchased from Sigma Aldrich. Potassium dichromate, Platinum(II) acetylacetonate Palladium(II) acetylacetonate, oleic acid, 1,2-hexadecanediol, 1-octadecene and citric acid were analytic grade from Sigma Aldrich Co., used as received.

Pt/Pd-Fe_3O_4 dumbbell-like nanoparticles (NPs) were obtained by a one-step method. In particular, before the synthesis, Platinum(II) acetylacetonate (0.1 mmol), Palladium(II) acetylacetonate (0.1 mmol), Iron(III) acetylacetonate (2 mmol), oleic acid (12 mmol), 1,2-hexadecanediol (10 mmol) and 20 ml of 1-octadecene were intimately mixed by sonication. After, the mixture was heated to 200 °C for 2 h under N_2 flow, and furtherly heated to reflux (~285 °C) for 1 h. The formed black-brown mixture was cooled to room temperature by removing the heat source. Pd-Fe_3O_4 dumbbell-like nanoparticles were also prepared following the same procedure but with only Palladium(II) acetylacetonate and Iron(III) acetylacetonate as precursors. To favour the dispersion of the NPs in the electrochemical medium a ligand exchange with citric acid (CA), was promoted (Sarno et al., 2017a; Sarno et al., 2018). The hydrophilic nanoparticles showed good dispersibility in water and remained stable for ~5 months.

The characterization was obtained by the combined use of different techniques. Transmission electron microscopy (TEM) images were acquired using a FEI Tecnai electron microscope operated at 200 KV with a LaB6 filament as the source of electrons, equipped with an EDX probe. XRD measurements were performed with a Bruker D8 X-ray diffractometer using CuKα radiation.

Due to the complexity of the HAs organic matter, the evolution of the reaction was determined by a global parameter, i.e. the total organic carbon (TOC) content of the solution (TOC sol), in mg/L. Samples were collected at different time points during the electrolysis. TOC was measured by using a Shimadzu TOC-V analyzer. To prepare the HAs solution, a purification step of commercial HAs was performed, similarly to the protocol of Arai et al. (Arai et al., 1986). The stock solution was prepared by dissolving commercial HAs in distilled water at pH 3.This solution was filtered through Whatman GF/F filter (0.7 µm as pore diameter). Then, HAs were precipitated by decreasing pH to 1.2 and the solution was centrifuged at 3000 rpm during 20 min.

All electrochemical tests were carried out during 9 h in a 100 ml batch electrochemical cell. The anode material was boron-doped diamond (BDD) thin-film onto a Nb substrate and the cathode material was a Pt foil. Electrodes were set up with a gap of 3 cm between the anode and the cathode.

For a typical electrochemical test, considering that in a natural water system, HAs are present in concentrations ranging from 0.1 to 200 mg/L (Kinniburgh et al., 1996), while, the concentration of Cr(VI) depends on the adsorption characteristics of the soil surfaces, a solution containing an initial TOC concentration of 130 mg/L (TOC_0) and 50 mg/L of Cr(VI) (e.g. tannery wastewater) was prepared. The pH solution was adjusted using dilute H_2SO_4 or 1.0 M NaOH before electrolysis. After adding 1.0 g of Pd-Fe_3O_4 or Pt/Pd-Fe_3O_4 NPs, the electrolysis was initiated by switching on the direct current (DC) power supply under Galvanostatic condition. The solution was stirred at 300 rpm using a magnetic stirring bar coated with Teflon throughout the experiment. The aqueous samples were withdrawn for analysis at determined time intervals (20, 60, 120, 180, 240, 300, 360, 420, 480, 540 min).

3. Results and discussion

The morphological and structural characteristics of the NPs were determined by transmission electron microscopy (TEM) analysis. The results of the syntheses consists of nanoparticles with highly uniform size, that once deposited over a copper grid, tend to self-organize, see Figure 1. The dumbbell nanoparticles are characterized by a quasi-spherical Fe_3O_4 nanoparticles (about 10 nm diameter) and faceted Pt/Pd exposing their round section (diameter < 2 nm).

The crystal structure of the synthesized Pt/Pd-Fe_3O_4 was characterized by X-ray diffraction (XRD), see Figure 2. The spectrum shows the reflection characteristics at higher angle compared to the peak position of pure Pt, suggesting an alloy formation between Pt and Pd based on the substitution of the Pt lattice sites (Sarno et al.,

2017b). It is possible, also, to assign the typical peak at 30.4° (220), 35.4° (311), 43.2° (400), 53.7° (422), 57.4° (511) and 62.7° (440) due to magnetite (JCPDS Card No. 75-0033) (Sun et al., 2009; Xu et al., 2009; Ban et al., 2010; Ghandoor et al., 2012). The crystalline sizes measured by Scherrer's equation was found to be 9.8 nm quite close to the TEM particle size measured. It means that all the as-synthesized Fe_3O_4 nanoparticles are single crystal. The lattice parameter "a" and interplanar spacing dhkl (Sarno et al., 2016b) were found quite close to the standard lattice parameter of magnetite and relatively far from the one of maghemite, which indicates that the as-synthesized iron oxide particles are in magnetite phase (Xu et al., 2009).

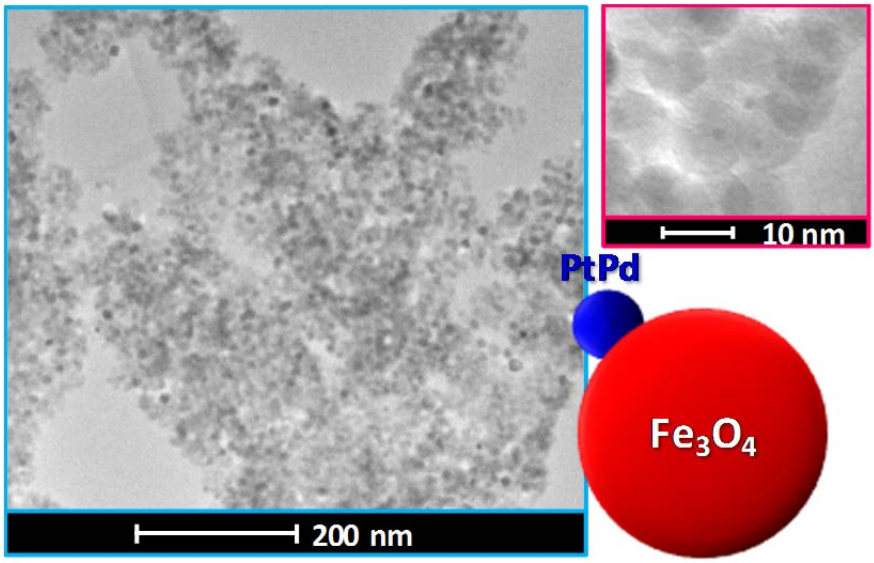

Figure 1: TEM images of Pt/Pd-Fe_3O_4 nanoparticles

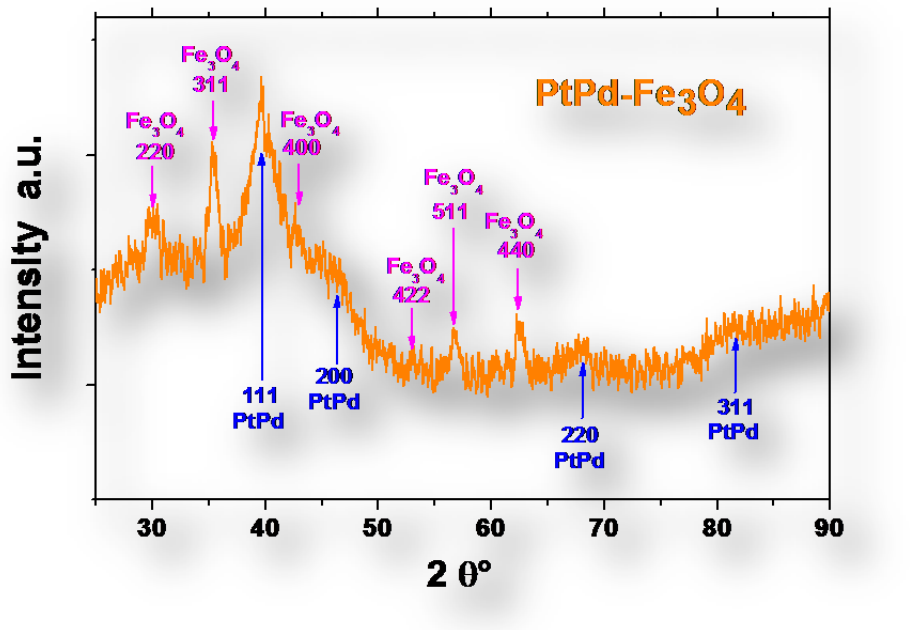

Figure 2: XRD spectrum of Pt/Pd-Fe_3O_4 nanoparticles

For HAs and Cr electrolysis: 30 mA, pH 3.0, 1.2 g of Pd-Fe_3O_4 or of Pt/Pd-Fe_3O_4, 130 mg/L HAs and 50 mg/L Cr (VI), were used. The results are shown in Figure 3a and 3b. Excellent removal efficiency for total Cr was shown, see Figure 3a. In particular, ~64% of total Cr was removed in 30 min, while ~95 % of total Cr was removed in 9 h. Moreover, the complete removal of Cr (VI) was achieved in 1.5 h. It was evident that ~95% of TOC was removed after 9 h electrolysis, indicating a quite complete mineralization to CO_2 of HAs, see Figure 3b. On the other hand, the behaviour shown by Pd-Fe_3O_4 NPs evidences the beneficial effect of Pt, probably due to an improved selectivity of the catalyst surface to form H_2O_2 instead of H_2 combustion (Sterchele et al., 2013), see the discussion below. These results confirm the effectiveness of the electro-Fenton process in the simultaneous removal of HAs and Cr(VI).
The effect of pH was also evaluated. At 9 h the TOC values were 12 mg/L and 29 mg/L at pH 5 and pH 7, respectively. The same behaviour was observed for total Cr, for which more than 10 mg/L were observed after 9 hours of treatment at pH 7 (Cr (VI).

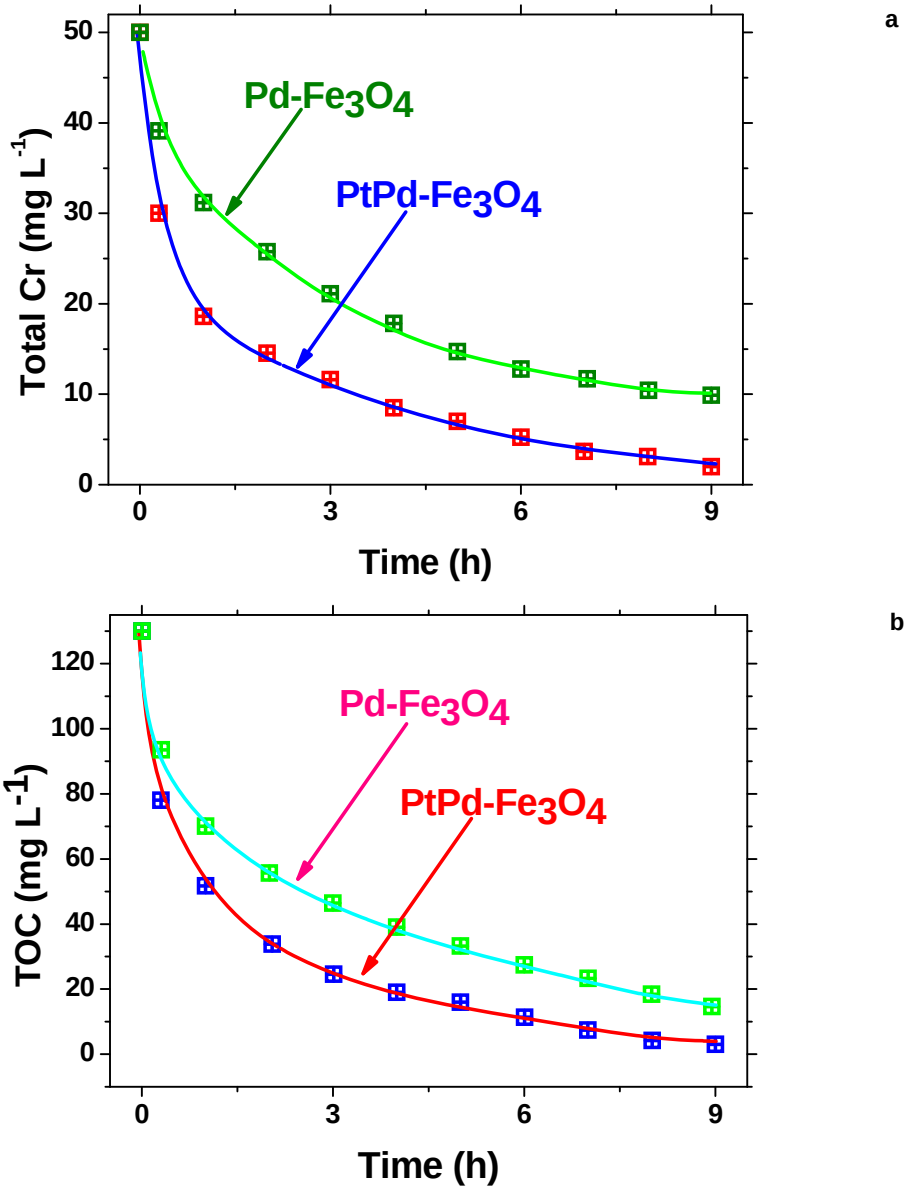

Figure 3: (a) Total Cr evolution as a function of time during electro-Fenton process. (b) TOC evolution as a function of time during HAs degradation.

Finally, a schematic mechanisms for the simultaneous removal of Cr(VI) and HAs is shown in Figure 4:

A. Due to electrolysis H_2 and O_2 gases are produced at the electrodes. On the other hand, $^{\cdot}OH$ can generate directly on the anode.
B. O_2, thank to an electron transfer, forms an highly oxidizing specie on the surface of Pt/Pd-Fe_3O_4.
C. H_2 and O_2 molecules on Pt/Pd surface are transformed in H_2O_2, and in presence of Fe^{2+} ions in $^{\cdot}OH$, highly able to oxidize organic compounds (Solano et al., 2016; Dirany et al., 2012; Florenza et al., 2016).
D. A recycle of Fe^{3+} to Fe^{2+} can be achieved thanks to atomic hydrogen on the catalyst surface.
E. Cr(VI) to Cr(III) occurs on the surface of Pt/Pd, too. In this step, $^{\cdot}OH$ can be also generated.
F. Cr(III) is removed by the deposition of chromite ($FeCr_2O_4$) from the solution phase.

The high efficiency of our nanocatalyst can be ascribed to the effective catalytic activity of the Pt/Pd nanoparticles during the steps (D), in which Pt presence probably favour the conversion of H_2 and O_2 to generate dissolved $^{\cdot}OH$ (Sterchele et al., 2013).

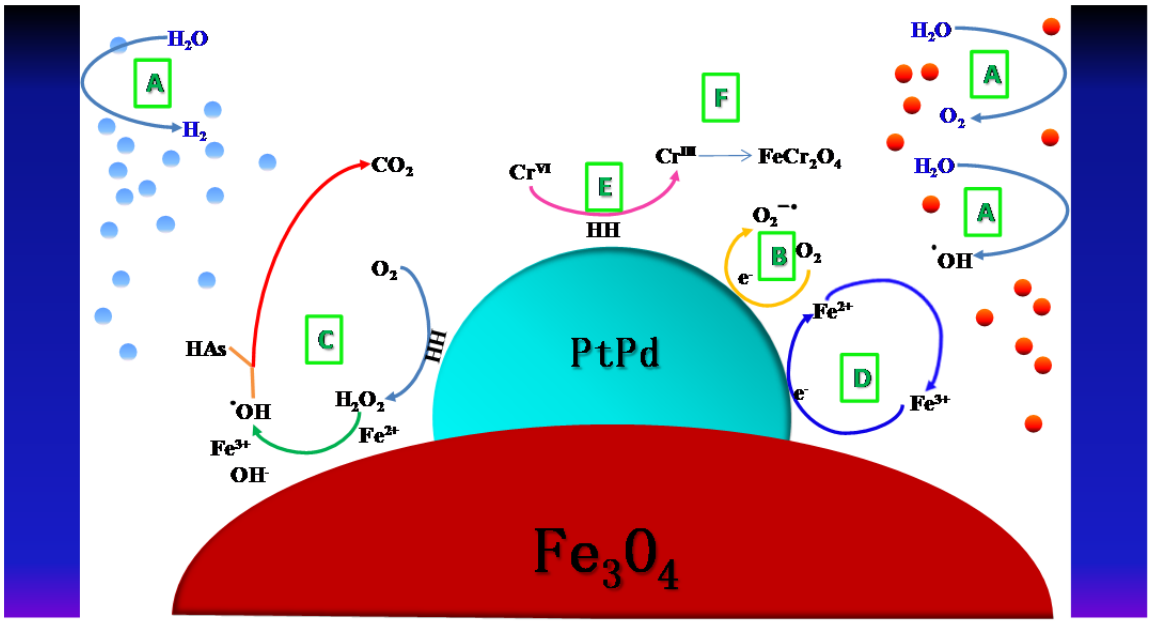

Figure 4: Schematic representation of the reactions mechanism.

4. Conclusions

A dumbbell-like Pt/Pd-Fe_3O_4 NPs nanocatalyst, consisting of faceted 2 nm Pt/Pd NPs on a quasi-spherical 10 nm Fe_3O_4 NPs, for the effective and simultaneous removal of HAs and Cr (VI), has been prepared by an efficient and facile one pot synthesis process. To favour the dispersion of the nanoparticles in the electrochemical medium a ligand exchange was designed and tested. The alloy formation between Pt and Pd, based on the substitution of the Pt lattice sites, was confirmed by XRD analysis. The magnetite crystalline sizes, measured by Scherrer's equation, was found to be 9.8 nm quite close to the TEM particle size measured. The electron transfer and hydrogen atom transfer were found the fundamental aspect during HAs and Cr(VI) removal. A comparison with Pd-Fe_3O_4 catalyst is also reported, highlighting the role of Pt in increasing catalyst selectivity. The homogeneous characteristics of the hydroxyl radicals produced by the electro-Fenton process determines their higher degradation efficiency on the respect of the anodic oxidation, suppling a more effective and safe way of H_2O_2 addition. The high efficiency of our nanocatalyst can be ascribed to the effective catalytic activity of the Pt/Pd nanoparticles, due to Pt presence, which favours the conversion of H_2 and O_2 to generate dissolved $^{\cdot}OH$ even more homogeneously distributed in the medium.

References

Arai H., Arai M., Sakumoto A., 1986, Exhaustive degradation of humic acid in water by simultaneous application of radiation and ozone, Water Research, 20, 885–891.

Ban C., Wu Z., Gillaspie D.T., Chen L., Yan Y., Blackburn J.L., Dillon A.C., 2010, Nanostructured Fe_3O_4/SWNT electrode: binder-free and high-rate Li-Ion anode, Advanced Materials, 22, E145-E149.

Celebi M., Yurderi M., Bulut A., Kaya M., Zahmakiran M., 2016, Palladium nanoparticles supported on amine-functionalized SiO2 for the catalytic hexavalent chromium reduction, Applied Catalysis B: Environmental, 180, 53–64.

Dirany A., Sirés I., Oturan N., Ozcan A., Oturan M.A., 2012, Electrochemical Treatment of the Antibiotic Sulfachloropyridazine: Kinetics, Reaction Pathways, and Toxicity Evolution, Environmental Science & Technology, 46, 4074–4082.

Florenza X., Garcia-Segura S., Centellas F., Brillas E., 2016, Comparative electrochemical degradation of salicylic and aminosalicylic acids: Influence of functional groups on decay kinetics and mineralization, Chemosphere, 154, 171–178.

Ghandoor H.E., Zidan H.M., Khalil M.M.H., Ismail M.I.M., 2012, Synthesis and some physical properties of magnetite (Fe_3O_4) nanoparticles, International journal of electrochemical science, 7, 5734-5745.

Kaya A., Onac C., Alpoguz H.K., 2016, A novel electro-driven membrane for removal of chromium ions using polymer inclusion membrane under constant D.C. electric current, Journal of Hazardous Materials, 317, 1–7.

Kinniburgh D.G., Milne C.J., Benedetti M.F., Pinheiro J.P., Filius J., Koopal L.K., van Riemsdijk W.H., 1996, Metal ion binding by humic acid: application of the NICA-Donnan model, Environmental Science & Technology, 30, 1687–1698.

Li L., Fan L., Sun M., Qiu H., Li X., Duan H., Luo C., 2013, Adsorbent for chromium removal based on graphene oxide functionalized with magnetic cyclodextrin–chitosan, Colloids and Surfaces B: Biointerfaces, 107, 76–83.

Sarno M., Cirillo C., Ciambelli P., 2014, Selective graphene covering of monodispersed magnetic nanoparticles, Chemical Engineering Journal, 246, 27-38.

Sarno M., Iuliano M., 2018, Highly active and stable Fe_3O_4/Au nanoparticles supporting lipase catalyst for biodiesel production from waste tomato, Applied Surface Science, in press. DOI: 10.1016/j.apsusc.2018.04.060.

Sarno M., Iuliano M., Polichetti M., Ciambelli P., 2017a, High activity and selectivity immobilized lipase on Fe_3O_4 nanoparticles for banana flavour synthesis, Process Biochemistry, 56, 98-108.

Sarno M., Ponticorvo E., 2017b, Much enhanced electrocatalysis of Pt/PtO_2 and low platinum loading Pt/PtO_2-Fe_3O_4 dumbbell nanoparticles, International Journal of Hydrogen Energy, 42, 23631–23638.

Sarno M., Ponticorvo E., Cirillo C., 2016b, High surface area monodispersed Fe_3O_4 nanoparticles alone and on physical exfoliated graphite for improved supercapacitors, Journal of Physics and Chemistry of Solids, 99, 138–147.

Sarno M., Ponticorvo E., Cirillo C., Ciambelli P., 2016a, Magnetic nanoparticles for PAHs solid phase extraction, Chemical Engineering Transactions, 47, 313-318.

Solano A.M.S., Martínez-Huitle C.A., Garcia-Segura S., El-Ghenymy A., Brillas E., 2016, Application of electrochemical advanced oxidation processes with a boron-doped diamond anode to degrade acidic solutions of Reactive Blue 15 (Turqueoise Blue) dye, Electrochimica Acta, 197, 210–220.

Sterchele S., Biasi P., Centomo P., Canton P., Campestrini S., Salmi T., Zecca M., 2013, Pd-Au and Pd-Pt catalysts for the direct synthesis of hydrogen peroxide in absence of selectivity enhancers, Applied Catalysis A: General, 468, 160-174.

Sun X., Zheng C., Zhang F., Yang Y., Wu G., Yu A., Guan N., 2009, Size-controlled synthesis of magnetite (Fe_3O_4) nanoparticles coated with glucose and gluconic acid from a single Fe(III) precursor by a sucrose bifunctional hydrothermal method, The Journal of Physical Chemistry C, 113, 16002-16008.

Sutton R., Sposito G., 2005, Molecular Structure in Soil Humic Substances: The New View, Environmental Science & Technology, 39, 9009–9015.

Trellu C., Péchaud Y., Oturan N., Mousset E., Huguenot D., van Hullebusch E.D., Esposito G., Oturan M.A., 2016, Comparative study on the removal of humic acids from drinking water by anodic oxidation and electro-Fenton processes: Mineralization efficiency and modelling, Applied Catalysis B: Environmental, 194, 32–41.

Wang L., Han C., Nadagouda M.N., Dionysiou D.D., 2016, An innovative zinc oxide-coated zeolite adsorbent for removal of humic acid, Journal of Hazardous Materials, 313, 283–290.

Wiszniowski J., Robert D., Surmacz-Gorska J., Miksch K., Weber J.-V., 2002, Photocatalytic decomposition of humic acids on TiO2: Part I: Discussion of adsorption and mechanism, Journal of Photochemistry and Photobiology A: Chemistry, 152, 267–273.

Xu Z., Shen C., Hou Y., Gao H., Sun S., 2009, Oleylamine as both reducing agent and stabilizer in a facile synthesis of magnetite nanoparticles, Chemistry of Materials, 21, 1778-1780.